ROTOR DESIGN FOR THE SSME FUEL FLOWMETER

Bogdan Marcu
Boeing
Rocketdyne Propulsion and Power

ABSTRACT

The present report describes the process of redesigning a new rotor for the SSME Fuel Flowmeter. The new design addresses the specific requirement of a lower rotor speed which would allow the SSME operation at 115% rated power level without reaching a blade excitation by the wakes behind the hexagonal flow straightener upstream at frequencies close to the blade natural frequency. A series of calculations combining fleet flowmeters test data, airfoil fluid dynamics and CFD simulations of flow patterns behind the flowmeter's hexagonal straightener has led to a blade twist design $\alpha = \alpha(\text{radius})$ targeting a *kf* constant of 0.8256. The *kf* constant relates the fuel volume flow to the flowmeter rotor speed, for this particular value 17685 GPM at 3650 RPM. Based on this angle distribution, two actual blade designs were developed. A first design using the same blade airfoil as the original design targeted the new *kf* value only. A second design using a variable blade chord length and airfoil relative thickness targeted simultaneously the new *kf* value and an optimum blade design destined to provide smooth and stable operation and a significant increase in the blade natural frequency associated with the first bending mode, such that a comfortable margin could be obtained at 115% RPL. The second design is a result of a concurrent engineering process, during which several iterations were made in order to achieve a targeted blade natural frequency associated with the first bending mode of 1300 Hz. Water flow tests preliminary results indicate a *kf* value of 0.8179 for the first design, which is within 1% of the target value. The second design rotor shows a natural frequency associated with the first bending mode of 1308 Hz, and a water-flow calibration constant of kf = 0.8169.

NOMENCLATURE

U	blade tangential velocity
Ca	fluid axial velocity
W	fluid relative velocity
α	blade stagger angle
β	angle of relative fluid velocity
i	flow incidence angle on the blade
C_D, C_L	drag and lift coefficients
ρ	fluid density
b	blade chord length
K_f	flow meter calibration constant for engine operation
K_{fw}	flow meter calibration constant determined from water flow test

1. INTRODUCTION

The Space Shuttle Main Engine uses a turbine type flow meter [3] to control the amount of fuel delivered to the engine and the mixture ratio between the fuel and oxidizer. The flow meter is located in a duct between the low pressure fuel pump discharge and the intake to the high pressure pump. The meter translates the volume flow of the liquid hydrogen based on its rotor speed and a calibration constant, denominated as K_f which relates the fuel volume flow rate to the rotor's rotational speed $K_f = 4*RPM/GPM$, where RPM is the rotor speed in rotations per minute and GPM the fuel volume flow rate in gallons per minute.

The original flow-meter design employed a flow straightener with a set of vanes forming channels with a square section, a configuration referred to as the "egg-crate" housing. Due to structural problems, this straightener was replaced by another design, with vanes forming a set of channels with hexagonal cross-section. In this new configuration, the flow meter rotor is mounted closer to hexagonal vanes, at 1 inch distance (previously, in the egg-crate straightener housing it was mounted at 2 inch distance). Over the years of SSME operation, a certain anomaly was observed in the flow-meter behavior [1]: at certain regimes, an apparent shift seems to occur in the K_f value, without a real change in the volume flow rate. This shift produces a false information in the SSME engine controller, generating a richer fuel-oxidizer mixture, and thus depleting the fuel reserve faster. The K_f shift phenomenon also appears to be associated with a fluctuation in the rotor's speed. Such fluctuation may be of high frequency, but since the rotation is only measured 4 times per one complete revolution, some aliasing phenomenon appears to occur in the measurements. Hence, the term of "aliasing" has been associated with the rotor speed fluctuations, occurring simultaneously with the K_f shifting.

Extensive work has been done to investigate these phenomena [2]. It was found that when the blade passes one of the wakes in the flow pattern generated behind the hex flow straightener, there is a momentary stall flow regime on the blade which slows down the rotor. The occurrence of successive such stalls may produce the K_f shifting phenomenon, associated with a high frequency oscillation in the rotor speed reffered to as "aliasing". The rotor wake interaction is stronger for the new hex housing due to the proximity of the rotor with respect to the straightener exit. Is was also found that the flow-meters displaying such shifting anomaly had rotor with small manufacturing errors, mainly small differences in the blade stagger angles from one blade to another.

Another issue of concern generated by the new hex housing is a strong symmetry pattern in the flow field behind it, especially 12N and 18N symmetry patterns. Such symmetry patterns generate an excitation with frequencies approaching the flow meter rotor blade natural frequency associated with the first bending mode (~830 Hz) if the rotor speed is approaching 4000 RPM. For this reason, the fleet flow meters have a limitation in speed at 3800 RPM in order to maintain a safety frequency margin. In many cases, this limitation precludes the SSME reaching 115% Rated Power Level.

2. DESIGN REQUIREMENTS

In order to resolve the issues related to the fuel flow meter operation, a reconfiguration of the meter has been decided upon. The hexagonal housing is being modified by cutting back the back face of the straightener vanes at a 27 degree angle. In this manner, the spacing between the vanes and the rotor is increased from 1.05 inches to 1.95 inches at the tip of the blade, while remaining 1.05 at the hub. Also, flow meter rotor is re-designed in a manner destined to achieve a lower rotational speed. The requirement is to achieve a maximum rotational speed of 3650 RPM at 115% SSME rated power level, for which the nominal fuel volume flow rate is 17,685 GPM. For this regime, the flow calibration constant must have the value $K_f = 0.8256$. A slightly lower value is admissible.

This report addresses the rotor re-design effort.

3. BLADE GEOMETRY

3.1. ORIGINAL BLADE GEOMETRY.

A complete set of manufacturing design details of the original rotor has been made available for the redesign project. However, while such design details allow for a proper part fabrication, they yield poor information for the purpose of inferring the fluid dynamics criteria on which the design is based. Since these criteria were not documented in the original design, they had to be reconstructed by processing the fabrication design data (blade sections defined at different radii) in combination with calibration data obtained from testing fleet rotors. Given the fact that a significant number of rotors were known to have small dimensional errors from manufacturing, data from a large number of rotors was necessary, with the hope that the statistics of the test results will generate mean values corresponding to a nominal design. Since the number of rotors with well documented test results was not large, data was selected for 10 rotors with good operational history (never recorded any anomaly in operation).

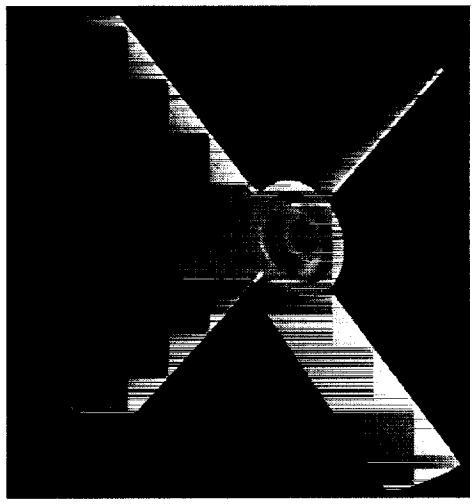

Figure 1. The flow meter rotor.

In order to organize a fluid dynamics design concept for the flowmeter rotor, one must understand a significant difference between a typical turbine destined to produce power, and the turbine flowmeter rotor at hand. A typical turbine rotor operates by organizing the working fluid flow within the channel formed between two adjacent blades in a way that maximizes loading, with a high degree of turning of the fluid, and with a strong interaction between the blades of the rotor. The flowmeter rotor or the other hand (shown in Figure 1), uses only 4 blades that operate practically independent of each other, as isolated rotating airfoils. If the rotor were to operate in a smooth, uniform incoming flow, its blades should operate at very small incidence angles at every radius. The situation is depicted in Figure 2. The incoming flow has a uniform axial velocity $\mathbf{C_a}$ and the rotor blade has the tangential velocity **U** as shown. Adding the two vector velocities results in the relative velocity with respect to the blade, **W**. The blade stagger angle α, is not aligned with the relative velocity angle β, as the relative velocity impinges on the blade's leading edge at a small incidence angle **i**. Since the blade profile is symmetric the small incidence angle is necessary for the flow around the airfoil to produce some lift, besides drag. Only the tangential components of the forces acting on the rotor blade are of interest. The blade will adjust its tangential velocity in a way that will produce a very small incidence angle **i** for which the tangential component of drag and rotor bearings

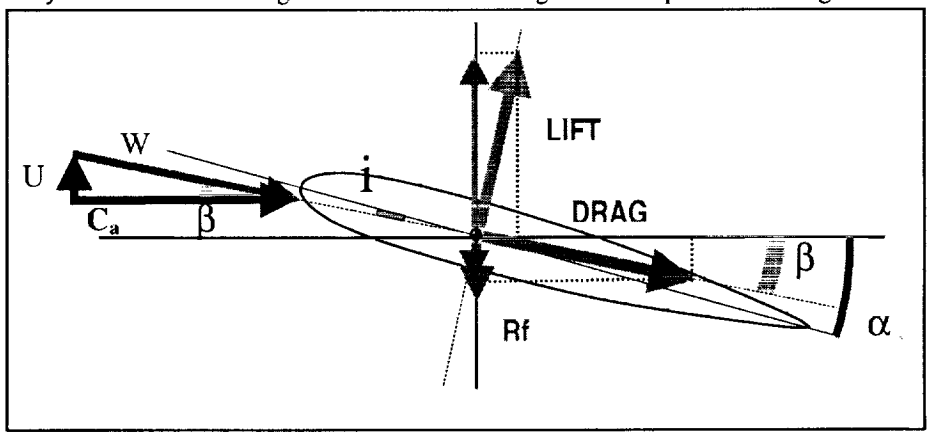

Figure 2. The blade load and force decomposition on the rotor blade.

friction resistance $\mathbf{R_f}$ will be compensated by the tangential component of lift. This model leads to a variable blade stagger angle which varies with the blade radius in a proportional manner if the small incidence angle is neglected, therefore we are seeking a relation of the form $\alpha = \alpha(\mathbf{R})$, where **R** is the blade radius. This relation depends on the required rotor speed at a given volume flow, and on the necessary incidence angle **i** at each blade radius. If we take under consideration the boundary layer development on the shroud and hub end walls, the incidence angle **i** then depends on the incoming flow axial velocity distribution with radius $\mathbf{C_a} = \mathbf{C_a(R)}$. Things are complicated more by considering the presence of the wakes in the incoming flow, which add a tangential dependency $\mathbf{C_a} = \mathbf{C_a(R,\theta)}$, where θ is a tangential angular coordinate. Such dependency further generates transient features that render the analysis too complex to obtain immediate useful results.

Therefore, let us consider an upstream flow that is characterized by a uniform axial velocity and no swirl. Based on this assumption, one could calculate a volume flow and a rotational speed of the original design rotor, at which the flow incidence **i** on the rotor blade is zero or close to zero at each radius. Is such a rotational speed is found for any given volume flow, the calculation verifies a free-vortex blade design. However, such calculation does not imply a stable rotation at the rotational speed calculated and no equilibrium of forces on the blade is assumed. This topic will be discussed in the next section.

By processing the original design blade profiles given at four radii, the blade stagger angles were obtained and used for the aforementioned calculation. The results show indeed a free vortex blade twist, with a theoretical flow calibration constant of $\mathbf{K_f} = \mathbf{8777}$, and close to zero incidence angles, as indicated in the following table, third column.

Table 1.

Blade Radius (% of blade height)	Blade angle α (degs)	Flow incidence angle **i** (for idealized, uniform upstream flow - degs)	Apparent flow incidence angle **i** (see Fig. 4) (calibration data – degs)
8.6	4.9	-0.0049	0.04
38.3	9.06	0.0016	0.07
68.0	13.13	-0.0011	0.10
97.7	17.06	0.0044	0.13

In operation, the upstream flow is not perfectly uniform, but distorted by wakes behind the hexagonal flow straightener, which together with the end-walls boundary layers generate an unsteady character of the incoming flow $\mathbf{C_a} = \mathbf{C_a(r,\theta,t)}$, in both tangential θ, and radial **r** directions. A good way to obtain an average flow calibration constant is to use all data points available from the calibration of the selected fleet rotors, and compute a calibration constant based on the mean square linear fit through the data. Figure 3 show this computation: the horizontal axis indicates the rotor speed measured in pips per second (a pip is a passage of one blade through a magnetic field of a sensor, hence 4 pips per rotation), while the vertical axis shows the liquid hydrogen volume flow through the meter, in gallons per minute. The dark line on the plot is a linear fit through the data points, yielding a flow calibration constant of $\mathbf{K_f} = \mathbf{8708}$, while the light colored line corresponds to the idealized case of perfectly uniform flow upstream and zero flow incidence on the blade at all radii, for which the calibration constant value is $\mathbf{K_f} = \mathbf{8777}$ as explained.

The difference between the two lines in figure 3 is very small, corresponding to calculated flow incidence angles shown in the fourth column of table 1. The largest flow incidence angle is calculated at 97.7% radius, a value of 0.13°. It is necessary to emphasize the fact that the flow incidence angles indicated in column 4 of Table 1 are not actual physical flow angles with respect to the blade, since the flow field at the blade leading edge is distorted by wakes and end-wall boundary layers as explained already. These incidence angles represent a model based on the forces and velocity diagram shown on Figure 2, which is intended to be used for redesign. The rational behind these values is as follows: *A dimensional average of the selected fleet rotors is very close to the original rotor nominal design, as the possible small*

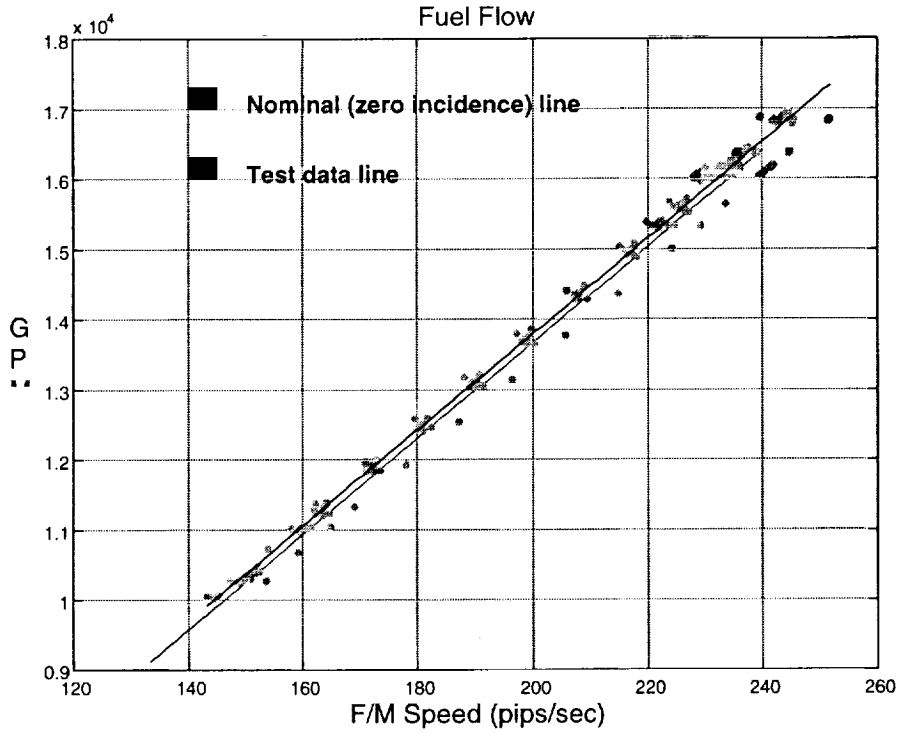

Figure 3. Calibration hot fire test data from fleet rotors, and linear fit of the data (dark line). The light colored line corresponds to the ideal case of uniform flow and zero flow incidence on the blade.

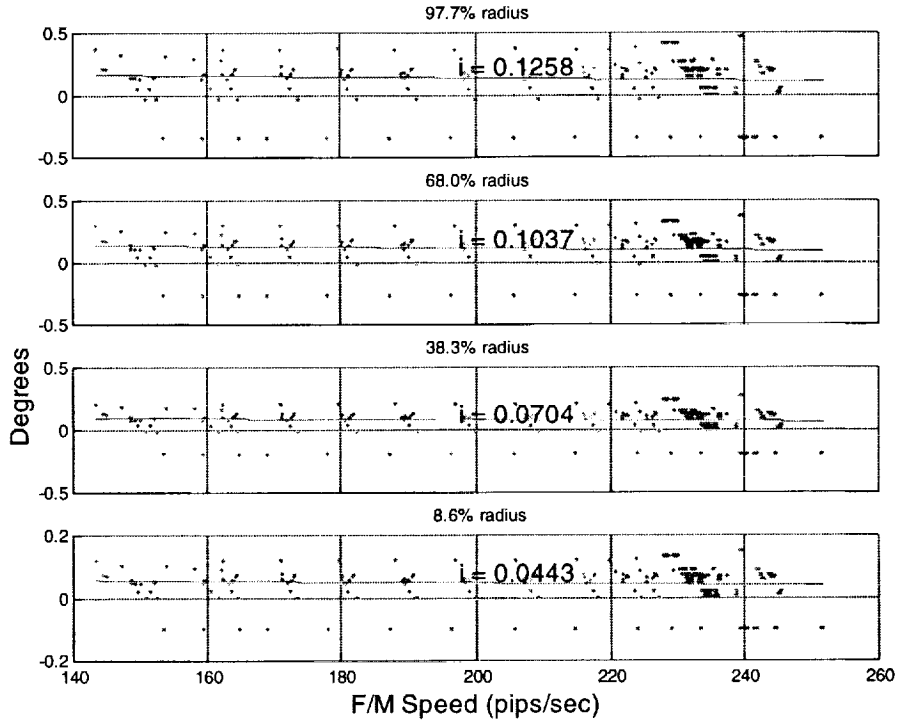

Figure 4. Apparent flow incidence angles at the radii where nominal blade design of the original rotor is specified. The line indicates a mean square linear fit through the data at each radius, while the numbers represent the average.

manufacturing errors statistically cancel out. The linearly fitted calibration data shows how fast does this virtually nominal rotor turn, for a given fluid volume flow. Assuming that this measured volume flow were perfectly uniform with no swirl, wakes or BL's present, and a rotor with nominal design were rotating with the measured speed (also from the linearly fitted calibration data), the flow incidence angles on the blade at the four specified radii would be those in column 4 of Table 1, denominated as apparent flow incidence angles.

The apparent flow incidence angle values listed in The apparent incidence angles listed in Table 1 are averaged over the entire pool of results shown in Figure 4. By knowing these values, a first approach to the design of a new rotor would be to simply retwist the blade at different stagger angles for the idealized case of zero flow incidences, then empirically add the apparent flow incidence angles to the blade stagger angles at each radius. However, data used for these calculations is obtained from the current flow meter configuration which uses the straight back hexagonal flow straightener. The wake flow structures behind the straightener has a significant influence on the measured flow calibration constants, and therefore a significant influence on the calculated apparent incidence angles. The new rotor design is destined to be mounted behind a cut-back hexagonal straightener, with a different wake flow pattern. For this reason, a more elaborate method is necessary for the new design, while using the apparent incidence angle presented in this section as a means of verification.

3.2. NEW BLADE GEOMETRY.

As specified in the previous section, by "blade geometry", in this study, one means a blade profile stagger angle variation with radius, i.e. a relationship of the form $\alpha = \alpha(\mathbf{R})$, where **R** is the blade radius and α is the blade angle (see Figure 2). The blade profile is symmetric at all radii, and the blades work independent from each other as rotating airfoils. The blade twist resulting from this relationship must provide a flow calibration constant of $\mathbf{K_f = 0.8256}$, as explained in section 1.

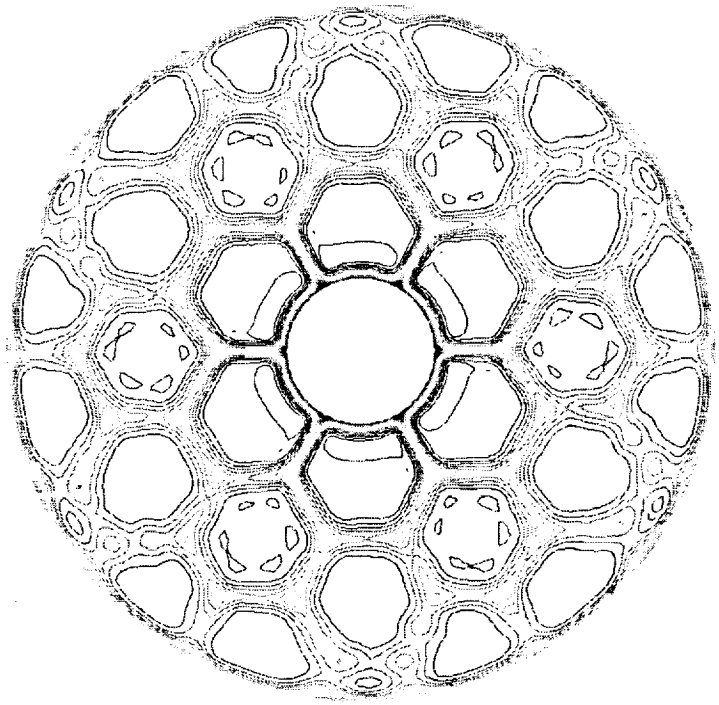

Figure 5. Axial fluid velocity field (CFD) behind the flow straightener, at a distance corresponding to the rotor blades leading edges locations.

The difficulty in choosing the new $\alpha = \alpha(\mathbf{R})$ design comes from the complex flow pattern generated behind the hexagonal flow straightener. Different studies [1,2] have shown that the proximity of the flow straightener to the rotor blade leading edges often generates anomalies in operations, such as shifts in the flow calibration constant associated with aliasing. Detailed CFD analysis [2] has shown the complexity of the upstream flow patterns and explained the $\mathbf{K_f}$ shift as resulting from a periodical quasi-stall phenomenon induced by the strong interaction between the wakes at the exit of the hexagonal flow straightener and the rotor blades. Such interactions were shown to diminish significantly with the spacing between the straightener and the rotor. For these reasons, the design of a new rotor has been conceptualized in conjunction with a modification of the hexagonal straightener, whose exit plane is being cut back at a 27° angle, increasing the distance from its exit to the blade from 1.0 to 1.9 inches at the tip of the blade. At the rotor hub, the 1 inch distance is maintained. Therefore the new blade design must account for the flow pattern behind the new straightener configuration in order to obtained a proper blade twist and provide the reduced rotor speed required.

The calculations presented in section 3.1 have shown that the original rotor blade design is essentially a free-vortex design. However, in order to obtain a precise rotor speed at a given volume flow, the designer must allow for a small alteration of the free-vortex blade twist, in order to account for the effects generated by the flow non-uniformity. Such effects are quantified by the apparent flow incidence angles also presented in section 3.1. In order to obtain such quantification for the cut-back straightener configuration both water-flow rotor test data with a prototype hex housing and CFD computations are used.

Figure 5 shows a CFD generated flowfield behind the cut-back hex straightener in the for of axial fluid velocity distribution $\mathbf{C_a}=\mathbf{C_a}(\mathbf{R},\theta)$, shown on a 120 ° sector in the transversal plane containing the rotor

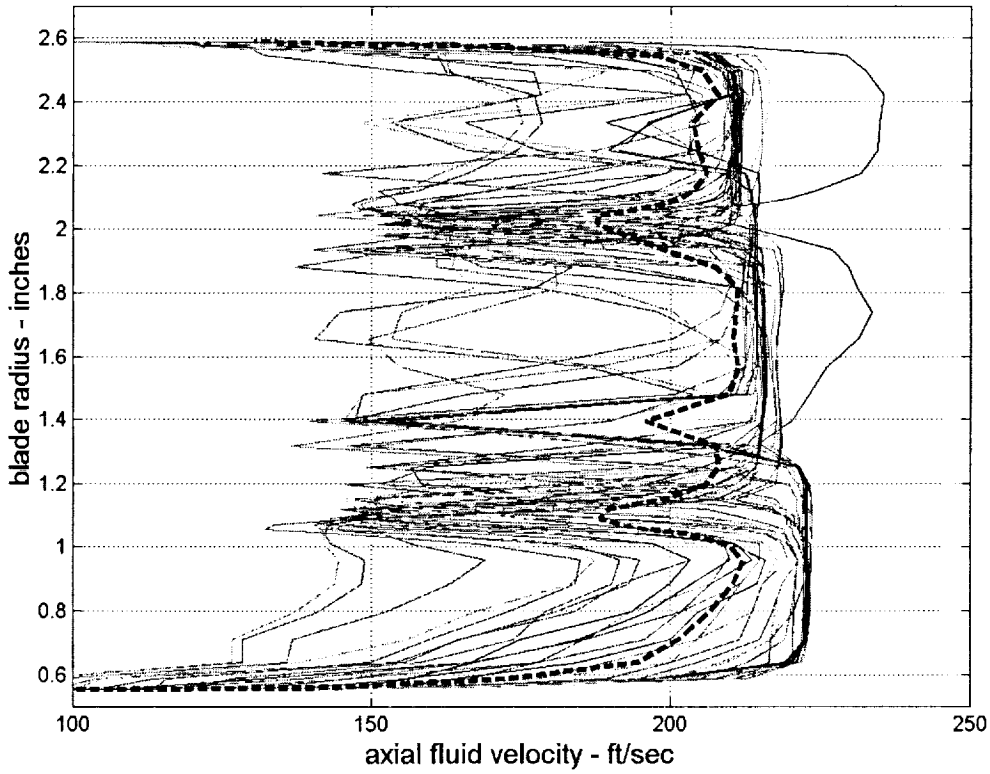

Figure 6. Radial distribution of the fluid axial velocity, plotted every 2.5 degrees for a 120 degrees sector. Data is extracted from the flow field shown in figure 5. The thick dotted line represents an average per one rotation in the tangential direction.

blades' leading edges. In this simulation, the rotor and its influence on the upstream flow is removed. Figure 6 shows, superimposed, several plots of the axial flow velocity distributions in the radial direction extracted every 2.5 degrees in the tangential direction from the flow field in figure 5. Basically these are the axial flow patterns that are "seen" successively by the rotor blade as it sweeps the flow field in its rotation. The average per one rotation in the tangential direction of the axial fluid velocity $\overline{C}_a = \overline{C}_a(R)$ is represented in Figure 6 by the thick dotted line . By examining this radial distribution of velocity one can understand that for a rotor blade twisted according to the free-vortex law, at any given instance, there are significant variations in fluid flow incidence angles **i** along the tangential direction, and at all radii. The incidence angle **i** can have positive as well as negative values within one complete rotation. Thus, at every moment, there are sections of the blade producing tangential forces in the direction of rotation, and other sections producing resistance. At each of these instances the flow around the entire blade is very complex, requiring significant resources to be resolved by real time CFD. The prohibitive cost of such resources in both equipment and man hours requires a different more practical approach.

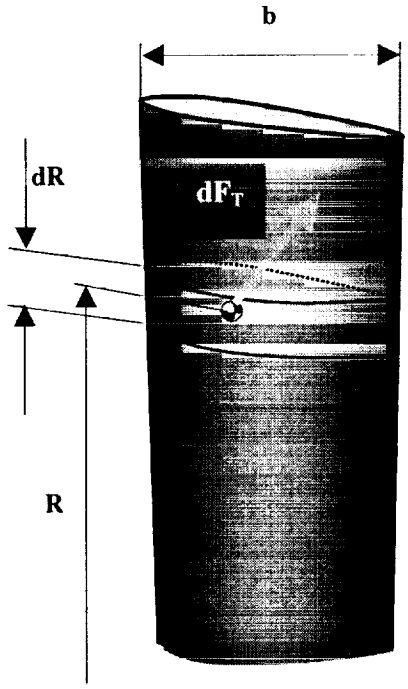

Figure 7. Force balance calculation on a rotor blade.

Figure 7 summarizes a calculation model that combines the aerodynamic principles expressed in Figure 2 with the available CFD data, and anchors them using test data. The rotor blade is divided in 32 horizontal bins as shown in the figure. Each bin produces, locally, either positive or resistive tangential force $\mathbf{dF_T}$, which, in turn, produces a positive or negative torque

$$\mathbf{dT = dF_T\, R} \tag{1}$$

The localized bin tangential force $\mathbf{dF_T}$, is a projection of the local drag and lift forces along the tangential direction (as shown in Figure 2) and a portion of the resistant bearings friction torque, which is small and can be neglected.

$$\mathbf{dF_T} = \frac{1}{2}\rho \mathbf{bdRW}^2 \times [\mathbf{C_L}(\mathbf{R})\cos(\beta(\mathbf{R})) - \zeta \mathbf{C_D}(\mathbf{R})\sin(\beta(\mathbf{R}))] \tag{2}$$

Here, **b** is the blade's width, **R** is the radius of the local bin, **dR** is the bin's radial width, $\beta(\mathbf{R})$ is the blade stagger angle, $\mathbf{C_L}$ and $\mathbf{C_D}$ are the local lift and drag coeficients — which depend on the local relative fluid velocity **W(R)** and local incidence angle **i(R)** — and ρ is the fluid density. For a given axial velocity distribution **Ca=Ca(R)**, a relative velcoity distribution **W=W(R)** results by vectorial addition with the tangential velocity $\mathbf{U(R) = R \times \omega}$, where ω is the rotor's rotational speed which achieves a stable, constant value when equilibrium is achieved on the blade:

$$\int_{R_{hub}}^{R_{tip}} \mathbf{dT} = 0 \tag{3}$$

The model is anchored for the **Ca=Ca(R)** distribution indicated by the average velocity profile in Figure 6, and the rotation resulting from several water flow tests of a cut-back hex straightener using three separate rotors which indicate a $\mathbf{K_f}$ value of **0.865**. The NACA 0016-64 airfoil $\mathbf{C_L}$ and $\mathbf{C_D}$ coefficient values are used in this calculations, since this NACA profile is closest to the original rotor blade profile from the literature available. It is important to note that in the model anchoring process one must account

empirically for several details associated with the physics of the problem at hand which are not accounted for in the model. Such details are: i) the nature of the working fluid is different from the fluid for which standard $\mathbf{C_L}$ and $\mathbf{C_D}$ are known, ii) the incident flow is characterized by intense fluctuations which alter the aerodynamic performance, iii) the three-dimensional character of the flow is neglected, locally, for each bin. The factor ς in equation (2) is the anchoring factor. The choice of placing this factor in association with the drag force term is based on the consideration that, given the flow fluctuations, it is to be expected that the drag on the blade profile be actually larger that the literature indicates, while lift forces will be smaller. A CFD analysis [ ] of the $\mathbf{K_f}$ shifting phenomenon seems to be indicating the same trend. However, the ς values do not reflect a quantification of drag amplification, and must be regarded as purely empirical values destined to anchor a model and be used in the design process.

Using the average **Ca=Ca(R)** velocity distribution in Figure 6, the measured $\mathbf{K_f = 0.865}$ flow coefficient is matched by choosing $\varsigma = \mathbf{32.0}$. Simulations show a very small sensitivity of the calculated $\mathbf{K_f}$ value with respect to ς, and therefore a good tuning capability of this parameter. Using $\varsigma = \mathbf{32.0}$, the new blade stagger angle $\alpha = \alpha(\mathbf{R})$ distribution is calculated based on a free-vortex blade twist altered by a small incidence angle distribution $\mathbf{i = i(R)}$, found by repeated iterations. Figure 8 shows the new blade stagger angle design, plotted together with the original blade stagger angle design for comparison. The difference between the old and the new design is small: only 0.84 degrees at the blade tip.

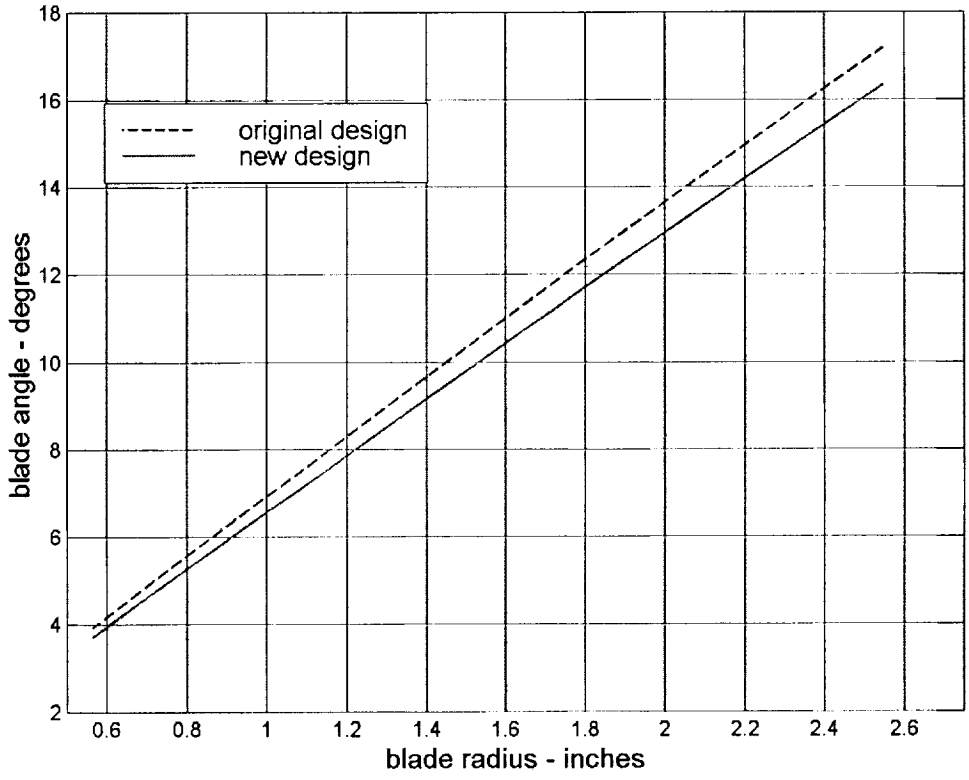

Figure 8. Blade stagger angle distribution

3.3. ROTOR DESIGN CONCEPT I

Having determined the new blade radial twist, the first design concept uses the original blade profile in shaping up a new blade using the new stagger angle distribution shown in Figure 8. The original blade design is given in the specifications at four radial stations (expressed in percentages of blade height in Table 1) by coordinate points x, y. The data has been processed numerically and the profile has been mathematically reconstructed based on circle elements (0.016 inch radius and 0.005 inch radius for the leading and trailing edges respectively.) and sets of third order polynomials. Figure 9 shows the reconstructed profile, which has a chord length of 0.747 inches, and a maximum thickness of 0.125 inches (16.7% relative thickness) at 40% of the chord length. For comparison, the NACA 0016-xx profile is plotted in the same figure.

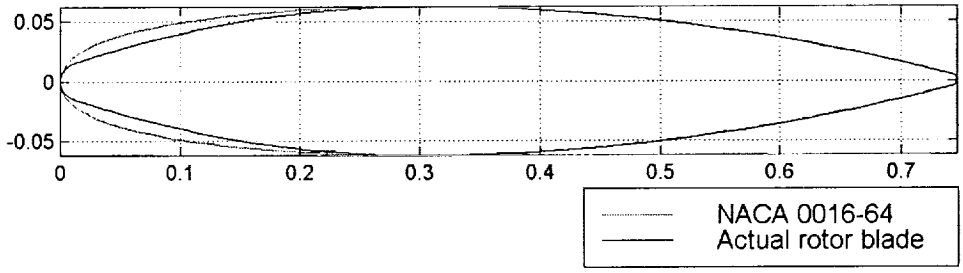

Figure 9. Rotor concept 1 and NACA 0016-64 airfoils. The rotor blade has been mathematically reconstructed from the x,y coordinates given in the original design documentation.

For the concept 1 rotor, the new blade natural frequency associated with the first bending mode is approximately 830 Hz, as expected. For a successful design, the rotor must not exceed 3650 RPM at a fuel volume flow of 17,685 GPM—which defines the regime at 115% SSME Rated Power Level—thus allowing for a 12% frequency margin with respect to the 12N symmetry excitation mode associated with the wake stracture behind the hexagonal straightener. The 3650 RPM is a slow speed for such high volume flow, rendering the design calibration coefficient $K_f = 0.8256$ very sensitive to any alteration in the blade stagger angle. For 3650 RPM, at the blade mean diameter the relative flow velocity has an average angle of 9.6°, while the blade's stagger angle is 9.9°. Given the blade profile accepted tolerance field for the original design of ±0.003 inches, a biased manufacturing within the 0.006 inch tolerance band as shown in Figure 10 can produce a stagger angle error of 0.46°, i.e. an error of 4.7%. This possible error places the rotor speed value in the 3475-3825 RPM range, which, for the right end of the range, not only reduces the frequency margin to 7.8% with respect to the 12N excitation, but also exceeds the 3800 RPM limit. For these reasons, the flow of information from the design concept to the manufacturing of the hardware must be carefully controlled.

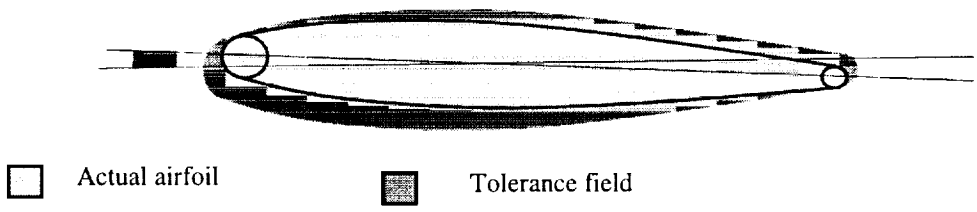

Figure 10. Stagger angle error due to biased manufacturing of the rotor airfoil, within the accepted tolerance band.

Such control is exerted by following the path of essential design information and ensure that minimum or no alteration of the original conceptual design geometry occurs. The blade geometry is imported into the solid modeling software via ASCII translation files. The airfoil geometry is therefore maintaining it's original mathematical definition. Furthermore, airfoil tolerance band is decreased from ±0.003 to ±0.002. The solid model of the rotors is further translated into ASCII translation file, and imported into the CNC software for manufacturing. Once in the manufacturing phase, information control of the geometry is weaker, and depends on the quality of the supplier's technology. For this reason, a feed-back loop into the information control is organized by extracting inspection-specific geometry data from the solid model, and inspect the final product. In this manner, the solid model becomes a reference element to which the final product is compared. The details of this information loop will be the subject of a future report.

The rotor concept 1 has been manufactured and water-flow tested, in conjunction with three types of flow straighteners: i) the orgiginal egg-crate straghtener, ii) the current design hex straightener and iii) the cut-back hex straightener. The water-flow calibration constants obtained are listed in Table 2.

Table 2. Rotor Concept 1 water-flow test results.

Type of upstream straightener	Water-flow calibration coefficient
Egg-crate	0.8180 ± 0.94%
Current design hex	0.8456 ± 0.7%
Cut-back hex	0.8179±0.18%

The water-flow calibration coefficient obtained for the cut-back hex straightener is $K_{fw} = 0.8179$, which is approximately 1% lower that the targeted value of 0.8256. Since the calculations were made for incompressible volume flows, this value should remain the same for engine operation . Nevertheless, in operation, the changes in Re number (a five fold increase) and nature of the fluid will slightly increase the value of the calibration constant, as the fleet testing experience shows. A quantification of this increase is difficult to predict.

3.3. ROTOR DESIGN CONCEPT 2.

The second design concept follows the same radial twist for the blade geometry, while targeting two additional objectives.

- An increase in the blade natural frequency associated with the first bending mode to 1300 Hz. For this frequency, there is a 16% frequency margin with respect to the excitation frequency associated with the 18N wake flow symmetry behind the hex straightener. Since 18N is the highest symmetry number, the blade natural frequency is above all excitation frequencies associated with the upstream flow in operation.
- An optimization of the flow around the blade in a manner that minimizes the effects of the strong wake structures at the hub— where there is only 1 inch separation between the rotor and the cut back hex straightener—and increases the role played by the flow around the upper half of the blade, located in a less perturbed flow field.

Both objectives are to be achieved by a tapered design of the blade geometry employing a variable blade chord length and a variable airfoil relative thickness from hub to tip. The design uses the modified NACA Four-digit series of airfoils whose relative thickness varies linearly from 24% at the hub to 13% at the tip. The chord length varies also linearly with radius, scaling the original design chord length by 109% at the hub and 100% at the tip. Figure 11 shows 8 radial sections of this design, by comparison to the original

profile. The final design was obtained after 14 iterations, each iteration consisting of a mathematical model, translation and import into a solid modeling software, followed by export into a stress and natural frequency analysis software. The manufactured rotor tested only 5 Hz difference from the predicted 1308 Hz natural blade frequency associated with the first bending mode.

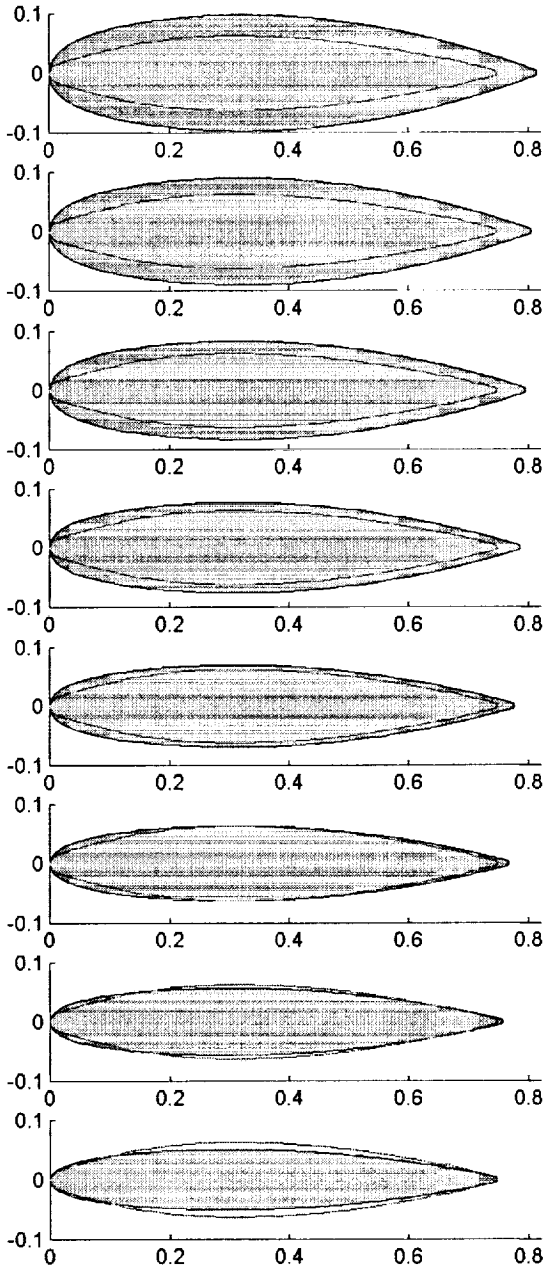

Figure 11. Rotor Concept 2 blade geometry shown at 8 equally spaced radial sections. The blade chord length varies linearly from 109% of the original chord length at the hub to 100% original chord length at the tip. Airfoil relative thickness varies linearly from 24% at the hub to 13% at the tip. Airfoils are modified NACA Four-digit series.

At the time of writing this report, only preliminary water flow tests of the second rotor design are available. The results are shown in Table 3.

Table 3. Rotor Concept 2 water-flow test results.

Type of upstream straightener	Water-flow calibration coefficient
Egg-crate	$0.8154 \pm 0.44\%$
Current design hex	$0.8436 \pm 0.1\%$
Cut-back hex	$0.8169 \pm 0.1\%$

The numbers are very similar to the results obtained for rotor concept 1, a bit slower. The same observations made at the previous section regarding the change in flow regime for engine operation should be noted here as well. Preliminary real-time measurements from the magnetic detectors show a very smooth rotation for concept 2 rotor.

CONCLUSIONS

A new rotor design has been conceptualized for the SSME fuel flowmeter, in conjunction with a modification of the hexagonal flow straightener destined to increase the spacing between the straightener vanes and the rotor's blades at the rotor's blade tip. The design requirement, essentially a slower speed, will allow safe operation of the SSME at 115% rated power level. The new design is obtained by a retwist of the rotor blades, following a calculated radial distribution of the blade stagger angle $\alpha=\alpha(R)$. Based on the same stagger angle radial distribution, two design concepts have been finalized, prototyped and water-flow tested. The first concept follows the new blade twist using the same blade profile as the original design. The second concept uses a tapered blade design which increases the blade natural frequency associated with the first bending mode to 1308 Hz, while optimizing the flow around the blade, generatgin a smooth operation. The water flow tests indicate a flow calibration constant within 1% of the targeted value.

ACKNOWLEDGEMENTS

The author wishes to acknowledge the contributions of William Bowling-Jr for the innovative solid modeling of the rotor geometry. Mr. Bowling's feed back and contribution to the control of the design information is essential to this project. The formulation of design requirements, management of design iterations, stress and blade dynamics feed back to the author is due to John Ubowski. The team efficient management and coordination as well as scheduling of the intensive water flow tests is due to Henry Loureiro.

Special thanks to Dr. Edward D. Lynch for providing the CFD flow field data behind the hexagonal straightener, and for the interesting discussions regarding the flow regimes and instabilities past the meter rotor blades.

REFERENCES

1. Fox. T.H., "Possible Mechanism for Flometer Oscillations Seen on STS-8", Mashall Space Flight Center Letter, April 9, 1984

2. Ascoli, E. et. al. "Application of CFD to Explain Stall Behavior of the SSME Flowmeter", AIAA paper 99-2458, presented at the 35th AIAA/ASME/SAE/ASEE Joint Propulsion Conference and Exhibit.

3. J.T. France, "The Measurement of Fuel Flow", AGARD Flight Test Instrumentation Series, Volume 3, NATO publication, 1972.

4. Schlichting, H. "Boundary Layer Theory", McGraw Hill, 1979

5. Abbot, I.H. and von Doenhoff, A. E.," Theory of Wing Sections", Dover , 1949.

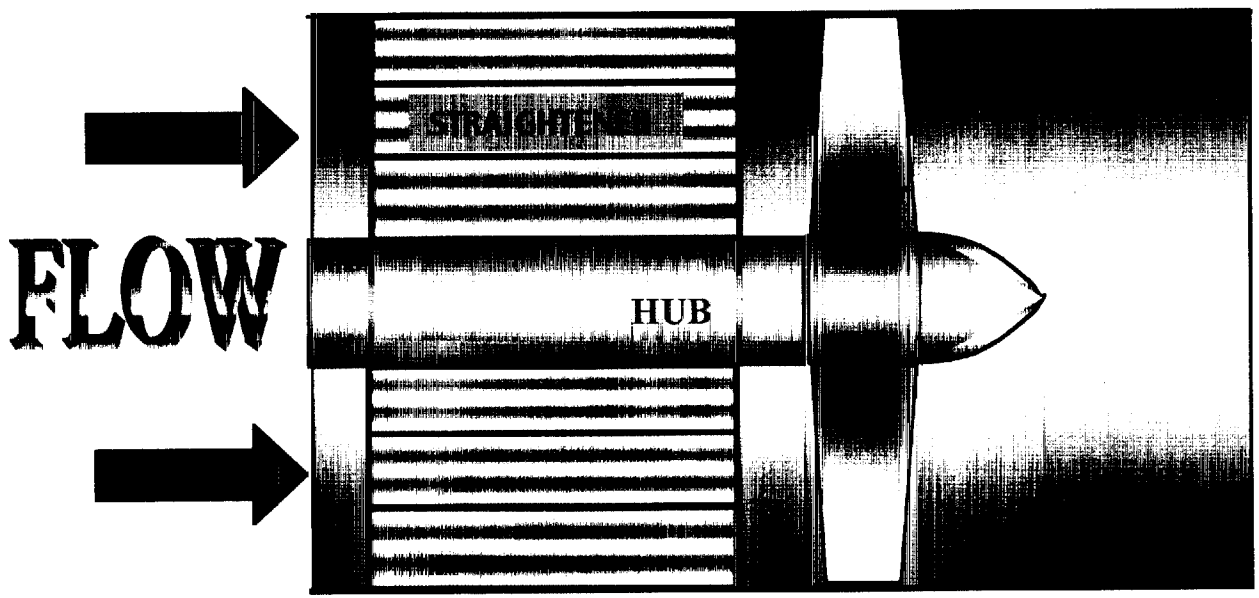

Slide 1

STRESS

- New hexagonal flowstraightener : flow wakes with 12N symmetry at rotor mean diameter
- Blade first bending mode natural frequency: 830 Hz $\rightarrow$ 4150 RPM
- Rotor Speed Limited to: 3800 RPM (760 Hz);
- Speed limit violation prevents some Low Pressure Fuel (LPF) ducts from operating at 109% and 111% of Rated Power Level (RPL)

ANOMALIES DURING OPERATION

- Shifts in value of the calibration coefficient, Kf
- Rotor Speed Fluctuations of Low Frequency (~ 25 Hz)

NO SAFETY ISSUES, PERFORMANCE ENHGANCEMENT

- Rated Power Level

Rated Power Level RPL	Fuel Volumetric Flow GPM	Rotor Speed RPM
67%	10300	2126
109%	16760	3459
115%	17685	3650

- RPM

$$K_f = \frac{4RPM}{GPM} \qquad \mathbf{K_f = 0.8256}$$

TASK 1. Determine the Nominal Design parameters of the existing rotor.

Available Information

- Design drawings from 1972
- Blade geometry airfoil defined at 4 radii (352 pairs of coordinates)
- Literature on the anomalies and related analysis

Original project and fluid dynamics calculations

- not available.

Test Data:

- hot-fire calibration data for 10 different rotors

$$K_f = \frac{4RPM}{GPM}$$

Blades work individually

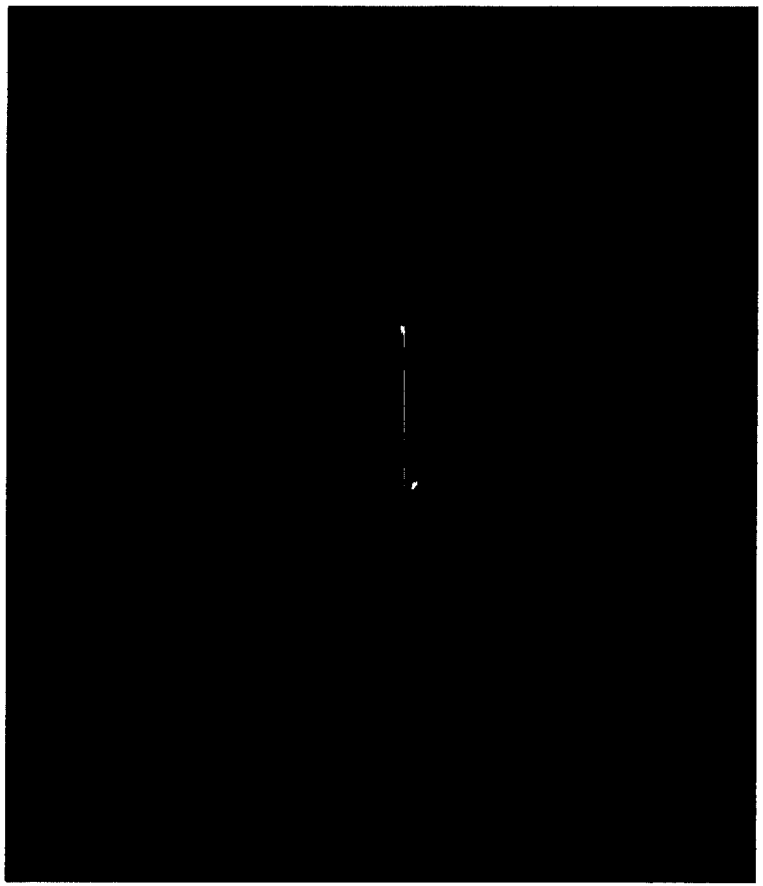

Velocity Triangles

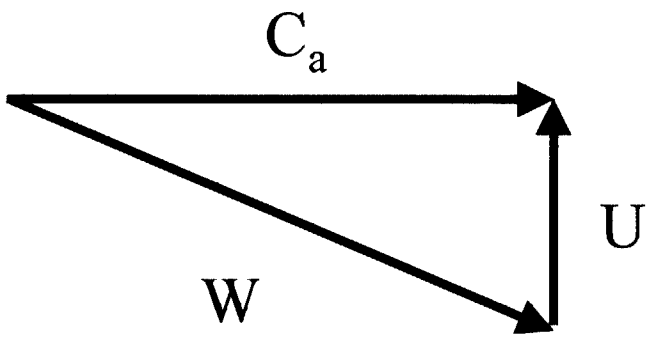

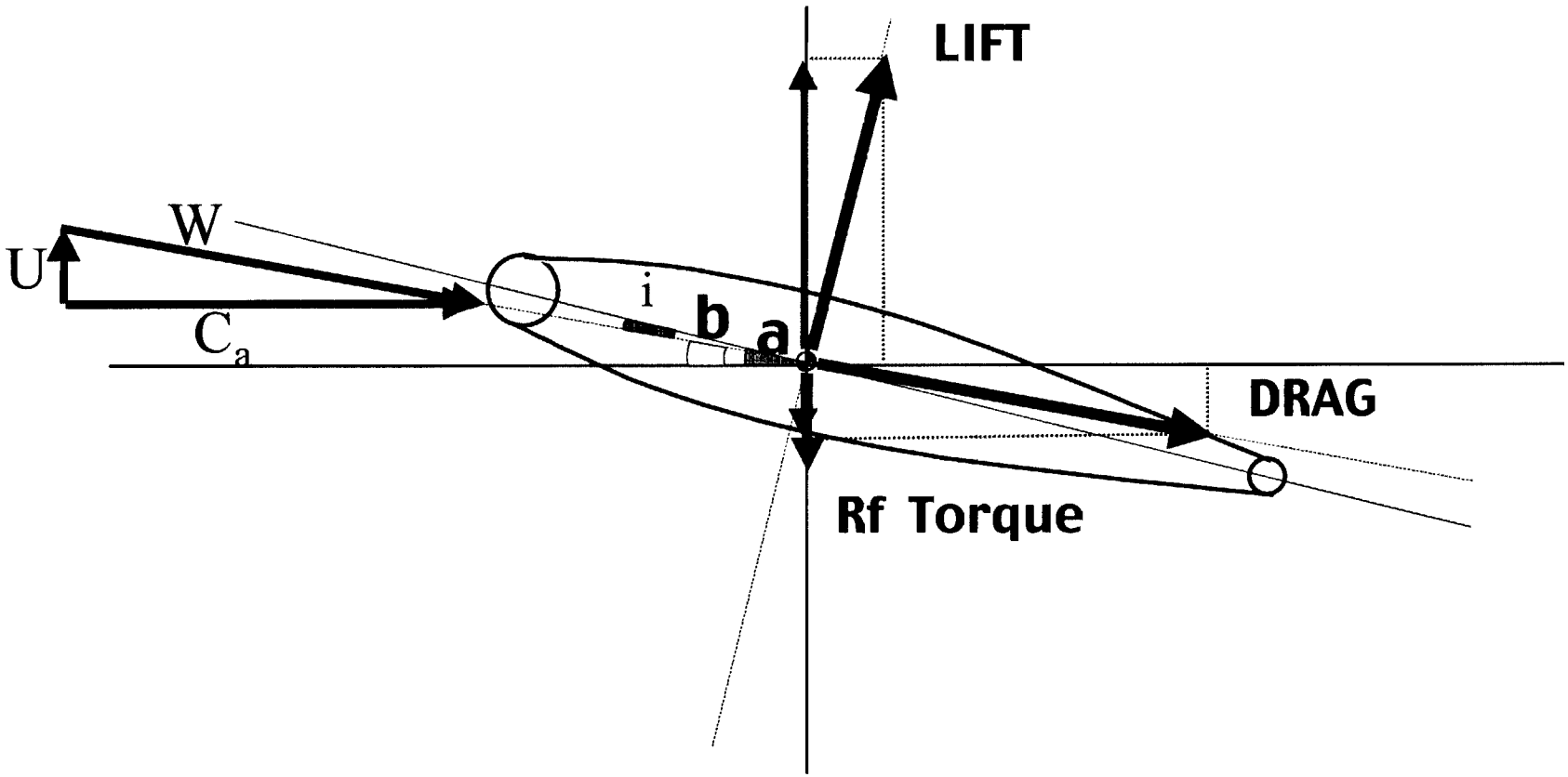
LIFT
W
U
C_a
i
b
a
DRAG
Rf Torque

Calibration diagram

Nominal:

- **0° incidence**
- **uniform upstream flow**
- **Kf = 0.8777**

TEST: linear fit

- **some incidence**
- **non-uniform flow**
- **Kf = 0.8708**

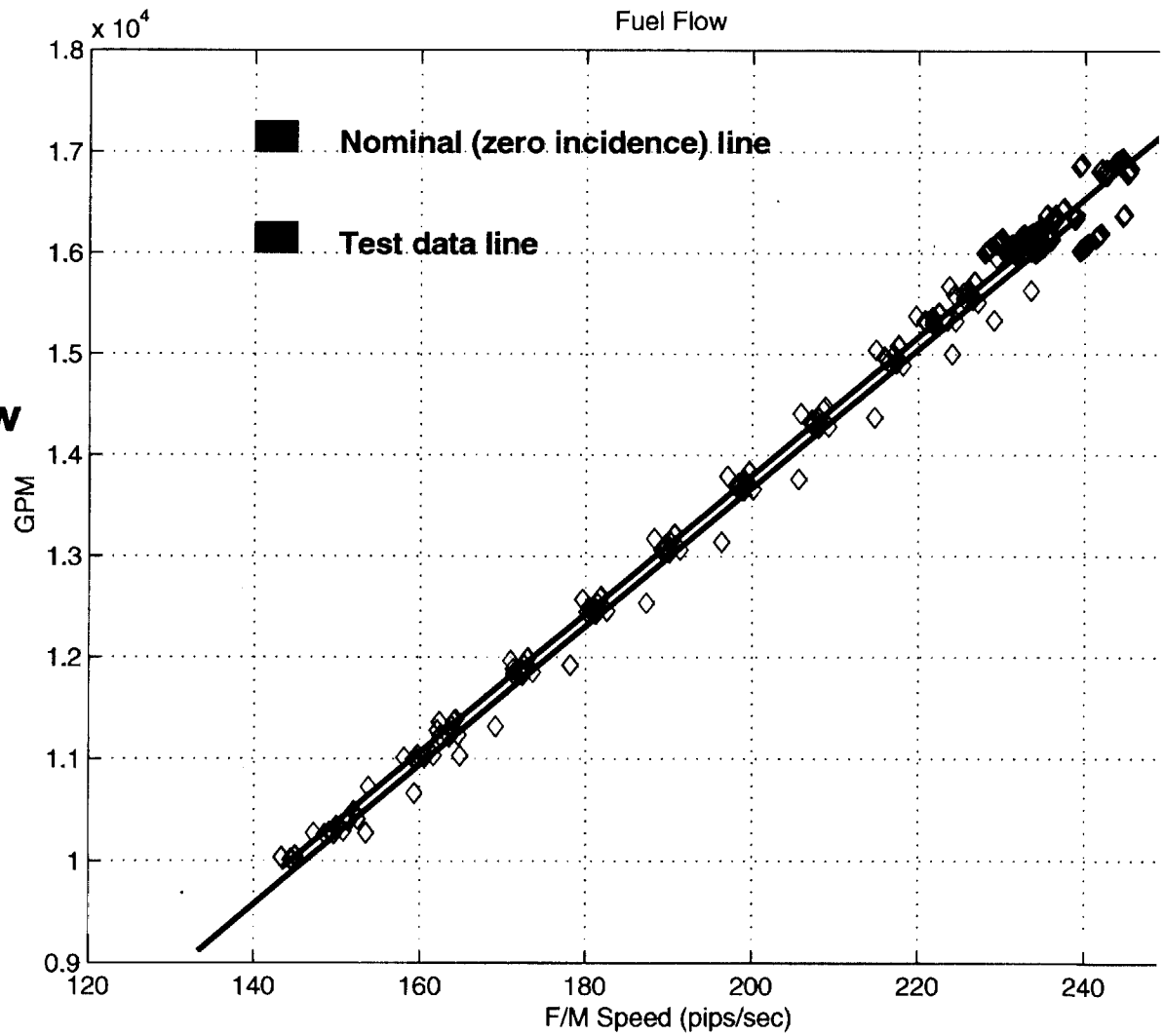

[redacted]

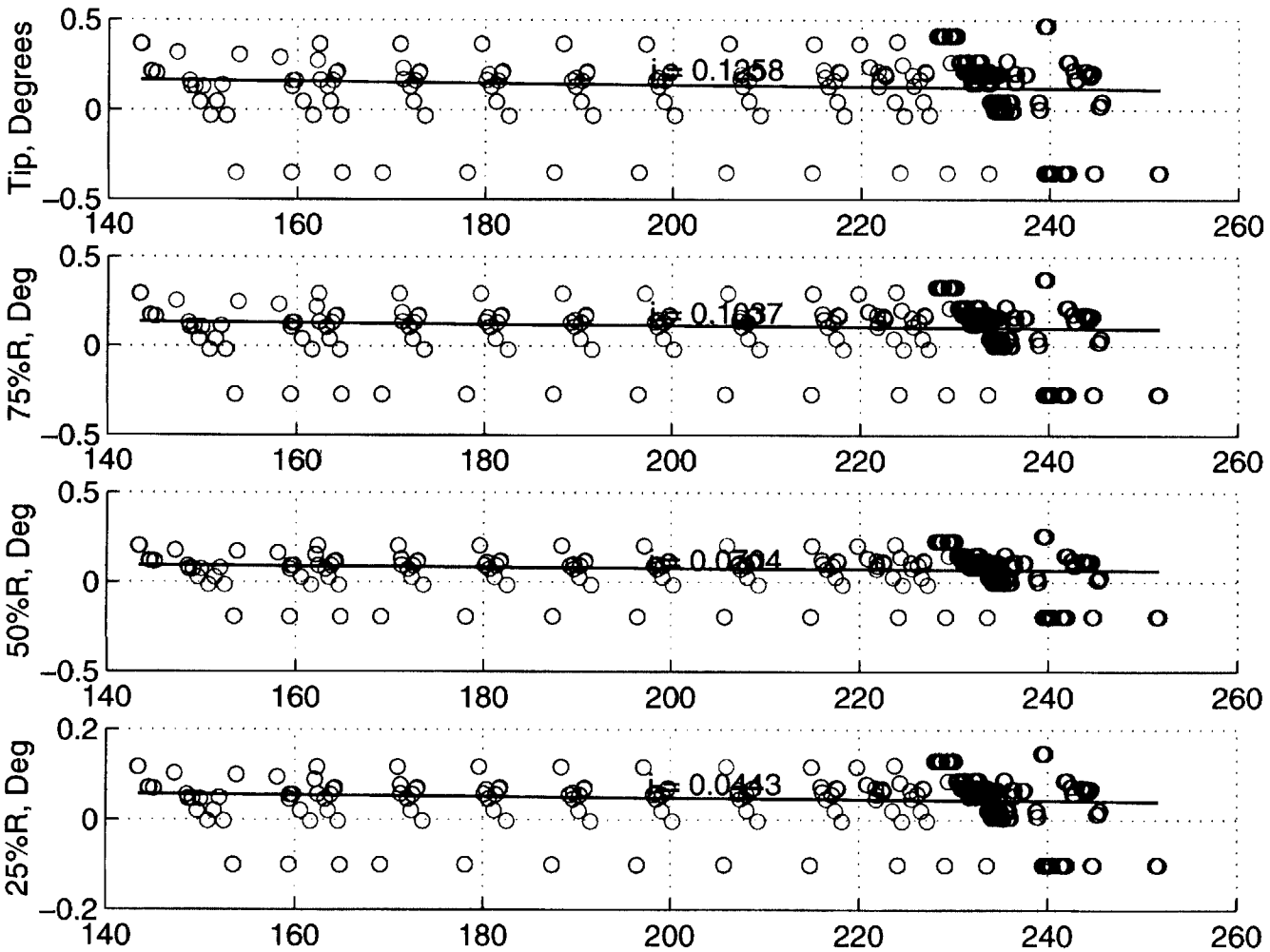

Slide 8

TEST
average calibration coefficient

Kf = .8708

REQUIRED
new design coefficient

Kf = 0.8256

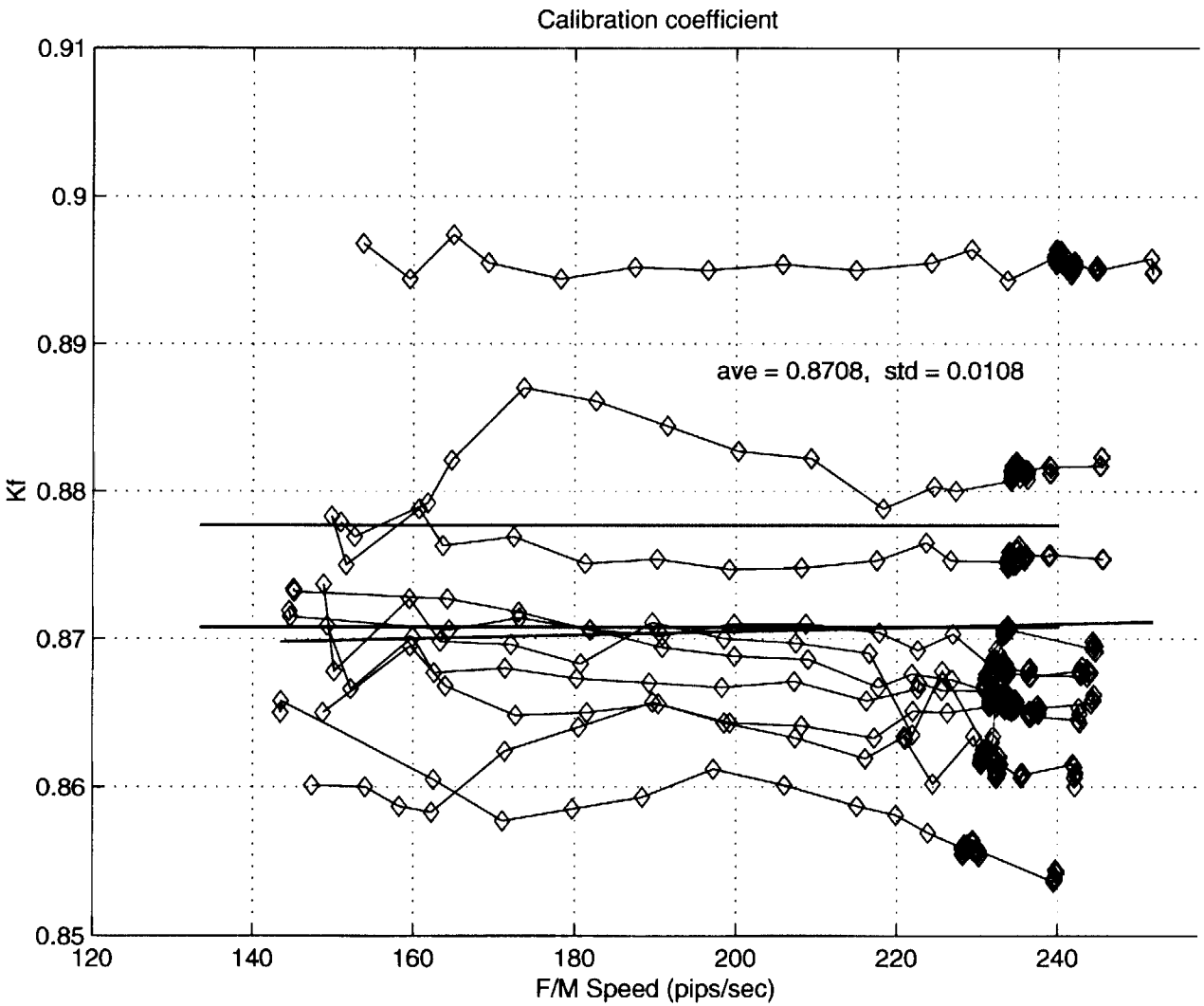

TASK 2. BLADE GEOMETRY CALCULATIONS

- Blade area divided into 32 bins
- Each bin produces torque:

$$dT = dF_T R$$

$$dF_T = \tfrac{1}{2}\rho b dr W^2 \times$$

$$\times [C_L(r)\cos(\beta(r)) - C_D(r)\sin(\beta(r)) - Rf]$$

- RPM is achieved at equilibrium $\int_{r_{hub}}^{r_{tip}} dT = 0$
- Uniform upstream flow

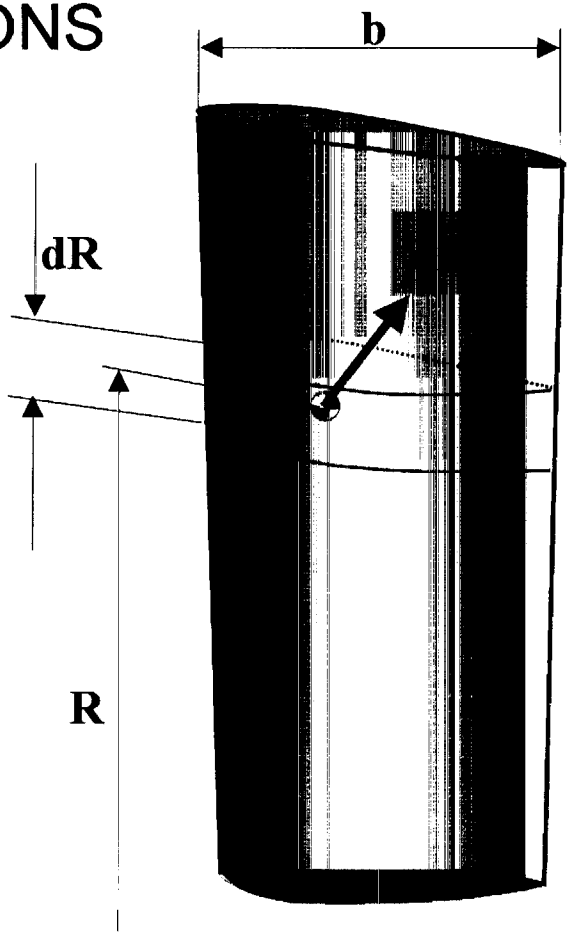

C_L, C_D, NACA 0012 - 64

Unknown Factors

- Upstream flow velocity field not uniform, BL, Wakes
- Effects of flow fluctuations on airfoil performance
- C_L, C_D data, measured in air, here LH_2

Some Possible Corrections

- Allow for a BL profile at the hub and tip walls
- Run calculations against test data, design empirical corrector
- Run calculations against CFD produced upstream flow field.

Refine the design

- Test preliminary design

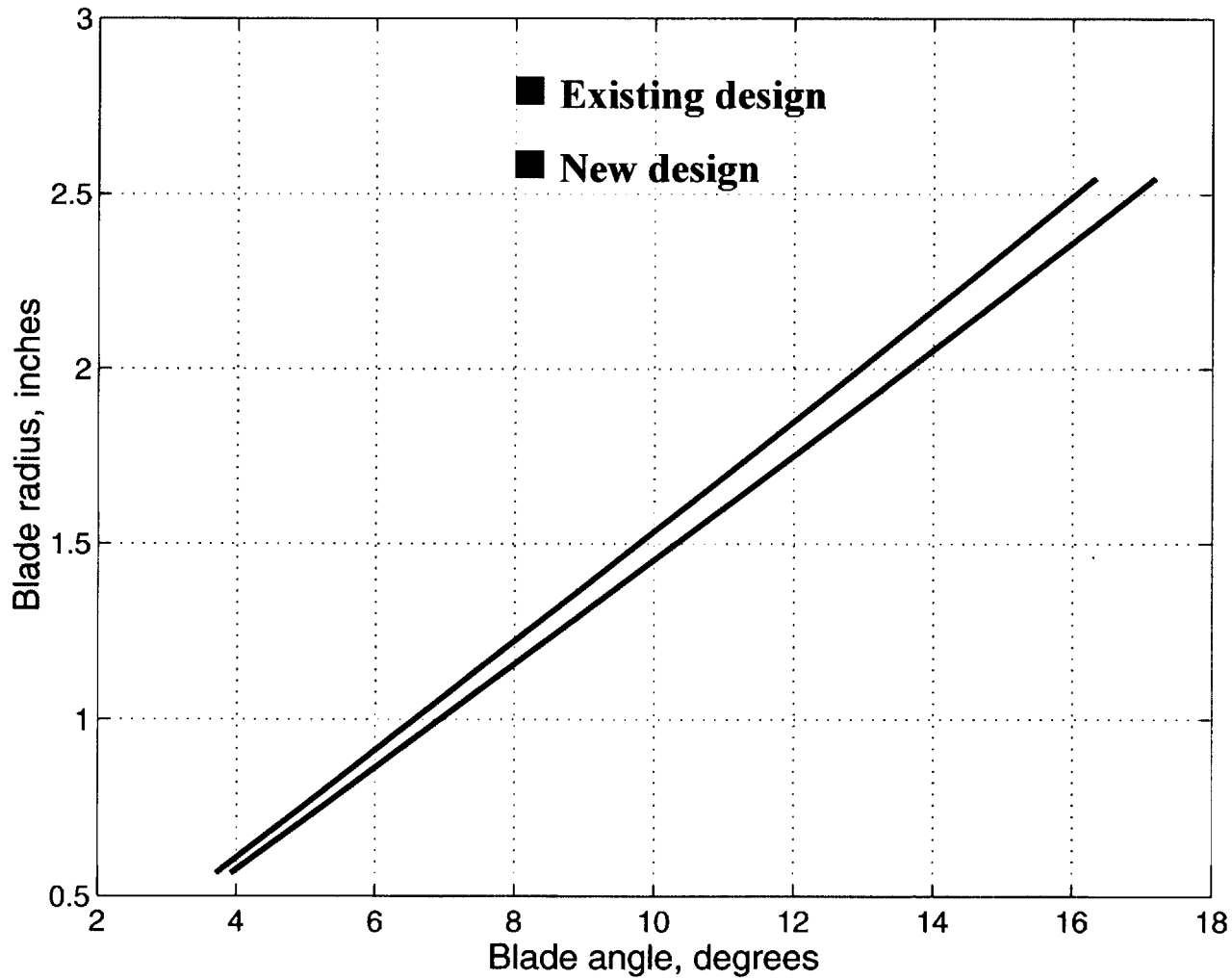
Existing design
New design
Blade radius, inches
Blade angle, degrees
3
2.5
2
1.5
1
0.5
2
4
6
8
10
12
14
16
18

Slide 12

TASK 3.

Concept 1.

- Using turbomachinery analysis, determine a new radial distribution of blade stagger angles

$$\alpha = \alpha(\text{radius}).$$

- Use the existing airfoil contour to generate a new blade geometry.

Concept 2.

- Based on the same $\alpha = \alpha(\text{radius})$, design a new blade geometry using a 10% larger airfoil contour. This allows
- thicker blade → increased natural frequency
- thicker LE → reduced sensitivity to incidence angle fluctuations
- longer chord

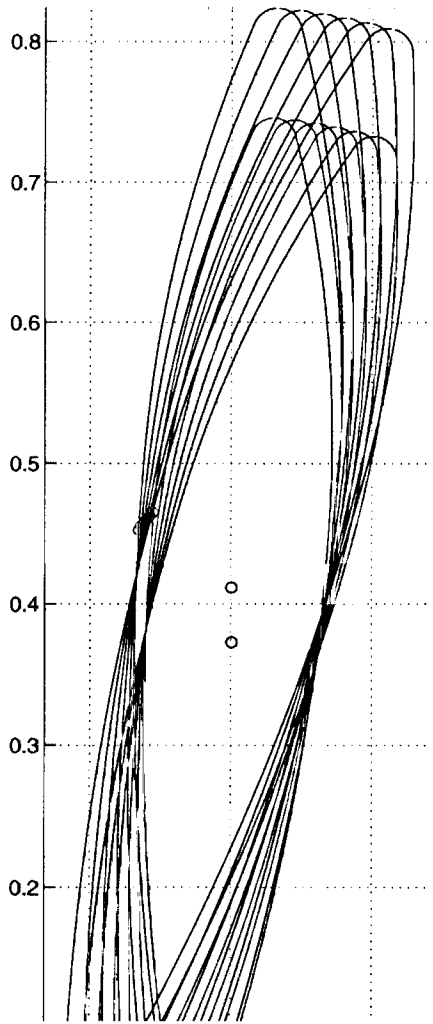

1. Non-uniformity in the upstream flow

CFD data

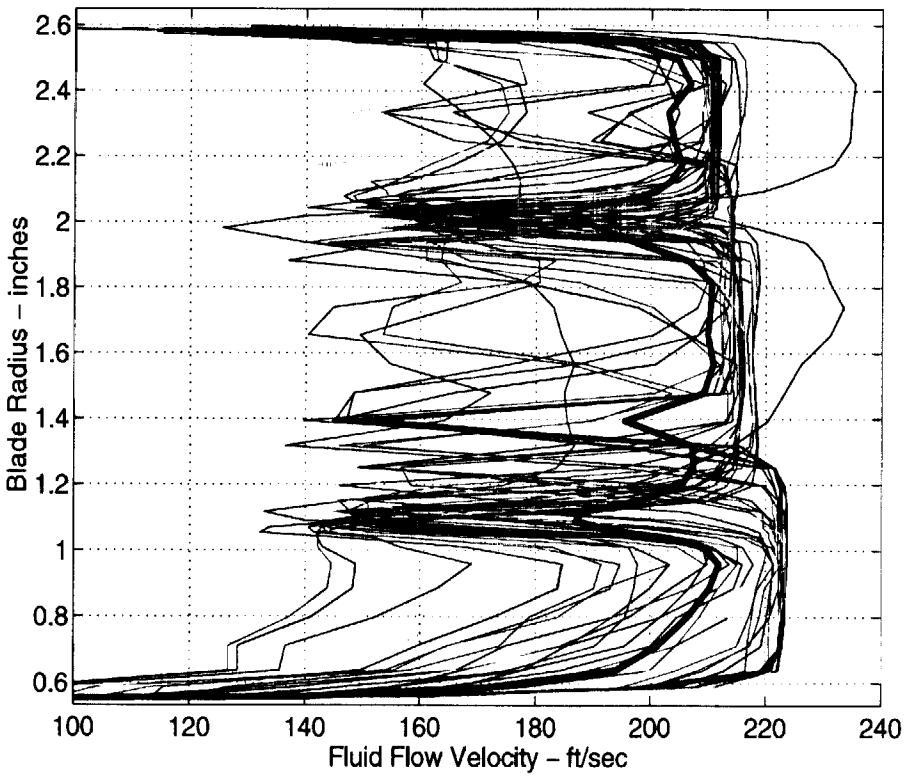

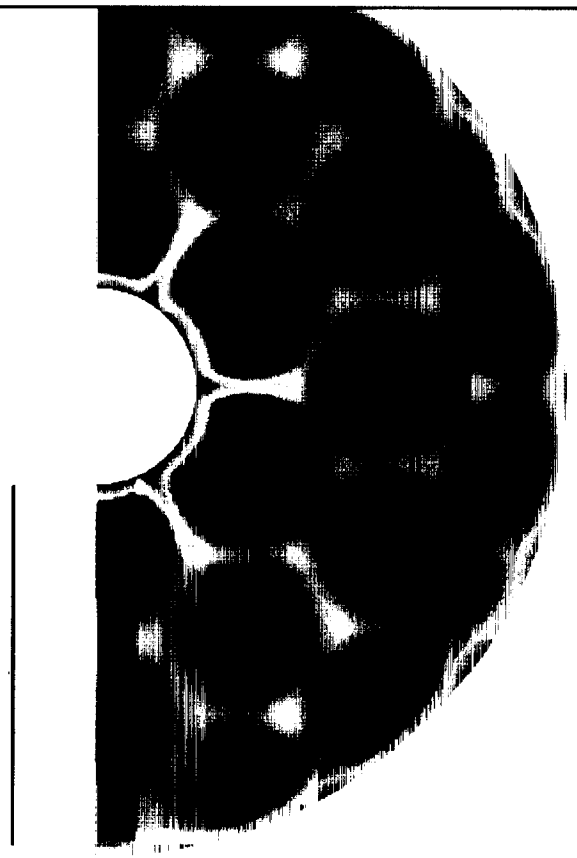

ft/sec

2. Manufacturing errors

- Within the currently accepted tolerance band (±0.003 in), the blade stagger angles can be deviated by as much as
  - **0.46°**
- This can lead to deviations is **Kf** values up to **2%.**

Corrections

- Existing airfoil accurately reconstructed mathematically
- Tolerance band restricted to ±0.002 in.

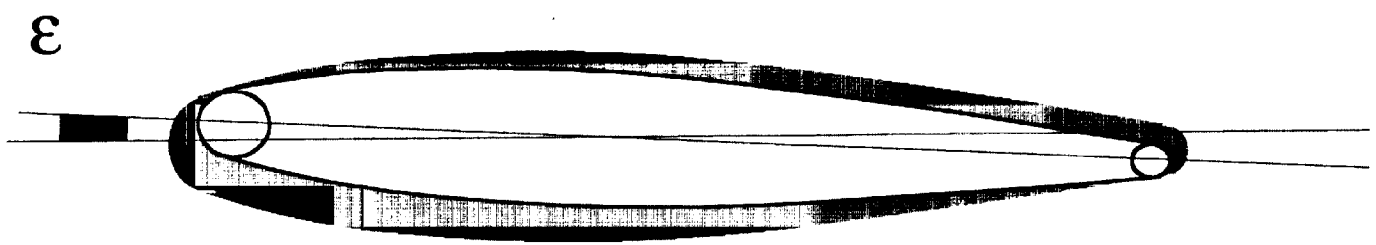

☐ Actual airfoil ■ Tolerance field

- **Blade re-twist using the calculated stagger angle**

$$\alpha = \alpha(r).$$

- **Use the original rotor blade profile (reconstructed)**

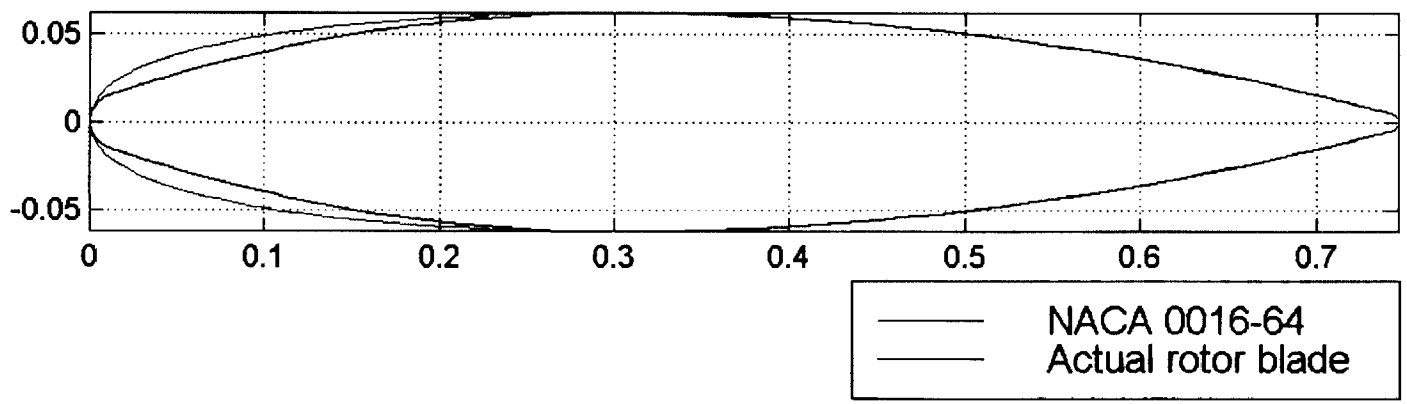

- **Blade re-twist using the calculated stagger angle**

$$\alpha = \alpha(r)$$

- **Use tapered blade geometry**
  - **linearly variable blade chord length**
    - **hub - 109% original chord**
    - **tip - 100% original chord**
  - **linearly variable profile relative thickness**
    - **hub - 24%**
    - **tip - 13%**
  - **NACA four digit series - modified (max. thick. at 40%)**

- **Increase in Blade natural frequency to 1308 Hz.**

Concept 2, Design stage II: NACA 4-digit airfoils, scaled

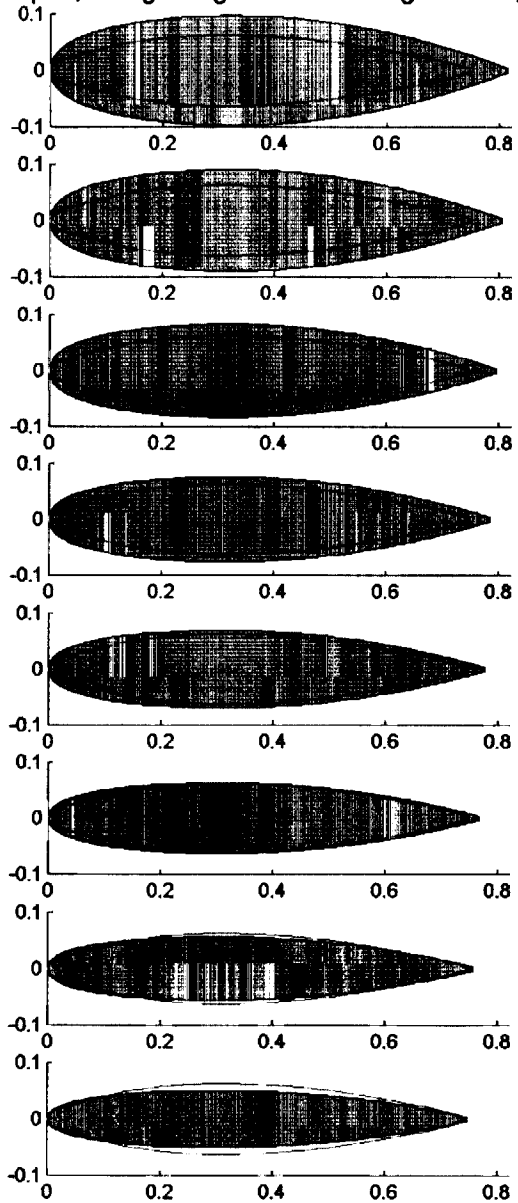

- **Rotor Concept 1**

Type of upstream straightener	Water-flow calibration coefficient
Egg-crate	0.8180 ± 0.94%
Current design hex	0.8456 ± 0.7%
Cut-back hex	0.8179±0.18%

- **Rotor Concept 2**

Type of upstream straightener	Water-flow calibration coefficient
Egg-crate	0.8154 ± 0.44%
Current design hex	0.8436 ± 0.1%
Cut-back hex	0.8169 ± 0.1%

- Rotor Concept 2 - chosen design
  - satisfies the speed requirements
  - smoother operation - Kf shifting possibility significantly reduced
  - allows safe SSME operation at RPL larger that 115%

- Verification on hot-fire engine test.